

THE DOUBLE CEPHEID CE CASSIOPEIAE IN NGC 7790: TESTS OF THE
 THEORY OF THE INSTABILITY STRIP AND THE CALIBRATION
 OF THE PERIOD-LUMINOSITY-COLOR RELATION

ALLAN SANDAGE

Mount Wilson and Palomar Observatories, Carnegie Institution of Washington,
 California Institute of Technology, and Mount Stromlo and Siding Spring Observatories,
 Research School of Physical Sciences, Australian National University

AND

G. A. TAMMANN

Astronomisch-Meteorologische Anstalt der Universität Basel,
 Binningen, Switzerland

Received December 17, 1968; revised February 17, 1969

ABSTRACT

Separate light curves in B and V have been obtained for the double Cepheid CE Cas a and CE Cas b . The components differ in color and luminosity, with component a brighter and redder than b by 0.07 mag in V and $B - V$. The observed ratio of the periods is $P_a/P_b = 1.15$, whereas the value predicted from $P\rho^{1/2} = Q$ using the photometric observations is $P_a/P_b = 1.16 \pm 0.04$, where the variation of Q across the instability strip is taken into account.

The effect on the period-luminosity-color relation of a variation of Q of the form $\Delta \log Q = h \Delta(B - V) + k \Delta \log P$ is shown to have no effect on our previous calibration.

Galactic Cepheids in clusters and associations give the P - L - C relations, $M_{(V)} = -3.425 \log P + 2.52 (\langle B \rangle^\circ - \langle V \rangle^\circ) - 2.459$, and $M_{(B)} = -3.425 \log P + 3.52 (\langle B \rangle^\circ - \langle V \rangle^\circ) - 2.459$, which reproduce the observed M_V values for the thirteen calibrating stars to within ± 0.064 mag average deviation. These equations represent a correction of -0.05 mag to the previous calibration. Expressions for the instability strip in the $(M_V, B - V)$ -plane for galactic Cepheids are given.

If perturbing effects, such as rotation, mass loss, and different main-sequence formation times, are excluded, the mass ratio of the more massive component to the less massive one must be less than $M_1/M_2 = 1.007$ if both stars are to be simultaneously within the Cepheid instability strip near $M_V \simeq -3$. This stringent requirement on the initial mass ratio will be relaxed if such perturbations affect the evolutionary tracks.

I. INTRODUCTION

Three Cepheids (CF Cas, CE Cas a , and CE Cas b) and an eclipsing binary (QX Cas) are members of the galactic cluster NGC 7790 (Sandage 1968*b*). Of these, the most remarkable is the double star CE Cas, both components of which are Cepheids with slightly different periods (5^d.14 for a and 4^d.47 for b). It seems likely that the stars form a physical pair. At a distance of 3200 pc, obtained later, the projected separation of the components is 8000 a.u., which is within the range of known binaries (cf. Kuiper 1935, 1951). (If it is assumed that each component has a mass of $5M_\odot$, the minimum orbital period is $\sim 2 \times 10^5$ yr.) If the pair has a common origin, it provides a unique and sensitive test of various aspects of the semiempirical description of the instability strip (Sandage 1958*a*; Kraft 1961*b*; Sandage and Gratton 1963; Fernie 1967*c*; Sandage and Tammann 1968 [hereinafter called Paper I]).

At least three tests appear to be possible. (1) Because the periods of CE Cas a and b differ, their mean densities cannot be the same if $P\rho^{1/2} = Q$. If both stars have nearly the same mass, their radii should be in the ratio $P_a/P_b = (R_a/R_b)^{3/2} (Q_a/Q_b)$. The prediction can be checked by observations of the color and luminosity differences between components a and b . Agreement would provide a test of the $P\rho^{1/2} = Q$ relation. (2) The individual colors and luminosities of a and b provide two additional tests of the current

absolute magnitude calibration of the period-luminosity-color ($P-L-C$) relation of Paper I. (3) The position of both stars within the instability strip provides observational information on the evolutionary tracks which feed the strip as calculated by Hofmeister, Kippenhahn, and Weigert (1964); Kippenhahn, Thomas, and Weigert (1965); Iben (1966*a, b*); and Forbes (1968).

Because these tests bear such a direct relation to the theory of evolution for giants and the validity of the $P-L-C$ relation, we have made a special effort to obtain colors and magnitudes for the separate components of CE Cas.

II. SEPARATION OF THE LIGHT CURVES

The angular separation of the eastern (a) and western (b) components is only about $2''.5$. Sufficiently accurate photoelectric photometry of the individual stars is not possible with any telescope, even in the best seeing. We therefore observed the combined light photoelectrically with the 60- and 200-inch telescopes at a number of epochs, using a diaphragm with a diameter of 25 seconds of arc which included both components. The data are listed in the first part of Table 1.

To obtain separate light curves requires knowledge of the intensity ratio of the components at each observed epoch. These data were found from light curves obtained by iris photometry from a long series of photographic plates on which the components appear to be well separated (225μ with a plate scale of $11''.06 \text{ mm}^{-1}$). The material consists of seventy-eight short-exposure plates taken at the prime focus of the 200-inch reflector with the mirror diaphragmed to 100 inches. The exposure times were generally 10 sec. After exclusion of twenty-two plates taken in poor seeing, there remained twenty-seven measurable B -exposures (103aO + GG13) and twenty-nine measurable V -exposures (103aD + GG11). The plates, their epochs, and quality are listed in Tables 1 and 2.

Each plate was measured three times, twice with the Becker iris photometer at Basel and once with the Sartorius iris photometer in Pasadena. Because the components of CE Cas are among the brightest stars in the cluster, very few comparison stars are available for calibration, especially in V . We were forced to use CF Cas and QX Cas as photometric standards. To ensure that light curves and phases were correctly known during the relevant 6-year interval, we made a special study of CF Cas and QX Cas, with the results given in Appendix A and B. The stars CF, QX, A, B, 95, 41, and E were used as standards, with the values adapted being those given either in the Appendices to this paper or by Sandage (1958*b*).

Despite the apparently clear separation of the components, crowding effects were clearly evident in the preliminary photographic data. The two sets of measurements with the Becker photometer agree well, showing a random difference of ± 0.02 mag per measurement. But these readings differ systematically from the Sartorius measurements by 0.110 mag (± 0.040) in B and 0.125 (± 0.040) in V such that the Sartorius readings are brighter. Iris readings are a complicated function of both image diameter and density. No two iris photometers respond equally to this function, and differences of the type encountered are to be expected in the presence of blending. Because the brighter readings are always suspect, we have corrected the Sartorius values to the system of the Becker photometer. Even then the resulting magnitude system is affected by blending, which was corrected as follows.

Light curves in B and V were constructed from the photographic data on the Becker system. Preliminary periods were adopted from the work of Payne-Gaposchkin and Gaposchkin (1963*a*), with adjustments to the epochs of maximum light to fit our observations. Examination of our early- and late-epoch photographic data, which spanned an interval of 2279 days, gave no evidence that these periods need correction.

The provisional light curves were converted into intensity units, and the intensity ratio of a to b was determined at each epoch of the photoelectric data. By this means, the

TABLE 1
PHOTOELECTRIC OBSERVATIONS OF COMBINED LIGHT AND THE ADOPTED SEPARATION INTO THE TWO COMPONENTS

Date	H.J.D. 2 430 000+	Combined Light			Instr	CE Cas a			CE Cas b			
		V	B-V	U-B		Phase ¹⁾	V	B	B-V	Phase ²⁾	V	B
1960 June 18/19	7 104.944	10.35	1.28	0.90	200"	274.410	11.01	12.27	314.638	11.20	12.51	1.31
20/21	106.975	10.16	1.09	0.74	"	274.805	11.13	12.48	315.092	10.73	11.67	0.94
Aug 16/17	164.008	10.32	1.20	0.77	"	285.898	10.91	12.10	327.824	11.26	12.47	1.21
17/18	165.000	9.91	1.02	0.70	"	286.091	10.69	11.77	328.046	10.63	11.60	0.97
Sept 23/24	201.936	10.15	1.17	0.81	"	293.276	10.87	12.07	336.292	10.94	12.07	1.13
24/25	202.916	10.33	1.26	0.90	"	293.466	11.03	12.32	336.510	11.14	12.37	1.23
27/28	205.738	9.93	1.02	0.69	"	294.015	10.64	11.67	337.140	10.73	11.73	1.00
28/29	206.673	10.20	1.12	0.80	"	294.197	10.84	11.94	337.349	11.07	12.22	1.15
1961 Jan 12/13	312.636	10.12	1.07	0.71	"	314.808	11.12	12.45	361.005	10.67	11.60	0.93
13/14	313.627	9.98	1.06	0.70	"	315.001	10.63	11.67	361.227	10.84	11.92	1.08
14/15	314.622	10.19	1.18	0.79	"	315.195	10.79	11.94	361.449	11.12	12.35	1.23
15/16	315.631	10.39	1.25	0.88	"	315.391	11.03	12.25	361.673	11.26	12.56	1.30
16/17	316.634	10.33	1.19	0.79	"	315.586	11.09	12.44	361.898	11.07	12.13	1.06
Aug 17/18	529.923	10.13	1.13	0.77	"	357.073	10.67	11.72	409.514	11.14	12.41	1.27
Sept 5/6	549.022	10.42	1.27	0.83	"	360.788	11.09	12.40	413.778	11.25	12.49	1.24
6/7	550.019	9.88	1.00	0.62	"	360.982	10.65	11.68	414.001	10.61	11.59	0.98
Oct 10/11	583.956	10.41	1.28	0.91	"	367.583	11.12	12.44	421.577	11.21	12.44	1.23
11/12	584.672	10.52	1.31	0.93	"	367.723	11.21	12.53	421.737	11.34	12.63	1.29
1962 Dec 26/27	8 025.633	10.11	1.20	0.83	60"	453.495	11.00	12.35	520.181	10.74	11.84	1.10
27/28	026.613	10.39	1.27	0.86	"	453.686	11.17	12.50	520.400	11.11	12.33	1.22
27/28	026.703	10.30	1.29	0.92	"	453.703	11.07	12.42	520.420	11.03	12.27	1.24
27/28	026.707	10.39	1.24	0.90	"	453.704	11.16	12.45	520.421	11.12	12.32	1.20
27/28	026.718	10.33	1.27	0.94	"	453.706	11.10	12.44	520.423	11.07	12.27	1.20
28/29	027.615	10.28	1.21	0.81	"	453.881	10.91	12.08	520.624	11.17	12.44	1.27
29/30	028.708	10.12	1.12	0.81	"	454.093	10.65	11.76	520.868	11.15	12.29	1.14
1963 Dec 10/11	374.699	10.08	1.10	0.75	200"	521.393	11.00	12.24	598.110	10.69	11.69	1.00
11/12	375.705	10.31	1.24	0.86	"	521.589	11.11	12.44	598.335	11.02	12.19	1.17

1) Phase of V(max) computed from epoch J.D.⊙ = 2 435 694.189 + 5.1410583n

2) Phase of V(max) computed from epoch J.D.⊙ = 2 435 695.586 + 4.4793014n

TABLE 2
 PHOTOGRAPHICALLY DETERMINED V MAGNITUDES ON THE ADOPTED
 PHOTOELECTRIC SYSTEM

Plate	H.J.D. 2 430 000+	Quality	CE Cas <u>a</u> ¹⁾		CE Cas <u>b</u> ²⁾	
			Phase	V	Phase	V
PH-1235-S	5 695.788	FG	0.311	10.935	0.046	10.695
1246-S	695.995	G	0.351	10.925	0.092	10.765
1257-S	696.805	G	0.511	10.965	0.273	10.805
1267-S	696.988	F	0.545	11.125	0.313	10.975
1291-S	698.745	FG	0.887	10.895	0.706	11.265
1302-S	699.000	G	0.936	10.895	0.762	11.295
1304-S	699.804	G	1.092	10.645	0.942	10.835
1311-S	699.995	G	1.130	10.645	0.985	10.625
1318-S	700.955	G	1.316	10.765	1.199	10.745
13-A	6 218.617	P	102.008	10.575	116.766	11.195:
3031-S	426.847	G	142.511	11.085	163.254	10.915
3039-S	429.991	FP	143.123	10.775:	163.956	10.795:
3046-S	436.761	F	144.440	10.935	165.467	11.055
3062-S	454.969	FP	147.981	10.705	169.532	11.145
3068-S	455.793	G	148.142	10.735	169.716	11.225
3073-S	456.013	G	148.185	10.775	169.765	11.335
3079-S	456.747	F	148.327	10.875	169.929	10.835
3090-S	457.018	G	148.380	11.015	169.989	10.665
3099-S	458.654	P	148.698	11.115:	170.355	10.845:
3333-A	758.955	F	207.111	10.775	237.397	11.125
3348-A	783.975	FP	211.977	10.635:	242.982	10.695:
3366-S	815.784	FG	218.164	10.655*	250.083	10.595*
3412-S	820.784	G	219.137	10.715*	251.200	10.875*
3423-S	847.718	G	224.376	11.045*	257.213	10.905*
3694-S	7 204.719	G	293.817	11.125	336.913	11.035
4033-S	969.788	F	442.632	11.185	507.714	11.295
4038-S	971.616	P	442.988	10.565	508.122	10.625
4049-S	973.639	G	443.382	11.055	508.573	11.265
4056-S	974.632	F	443.575	11.165	508.795	11.315

* Mean of three exposures on one plate.

1) Phase of V(max) computed from epoch $J.D._{\odot} = 2\ 435\ 694.189 + 5.1410583n$

2) Phase of V(max) computed from epoch $J.D._{\odot} = 2\ 435\ 695.586 + 4.4793014n$

light could be divided into the contribution due to a and that due to b , and then, by using the zero point provided by the photoelectric data, it could be converted back into magnitudes for a and b alone. These values were plotted against phase to produce a new light curve with an improved zero point. The procedure was repeated until convergence was reached.

The provisional photographic B -curves proved to be nearly correct even in the first approximation, but the combined photographic V -intensities were brighter by about 10 percent at all phases than the corresponding photoelectric intensities. Three approximations were needed to obtain the asymptotic shape of the B -curves; four approximations, to obtain that of the V -curves.

The final results are shown in Figures 1 and 2 where only the photoelectric values are

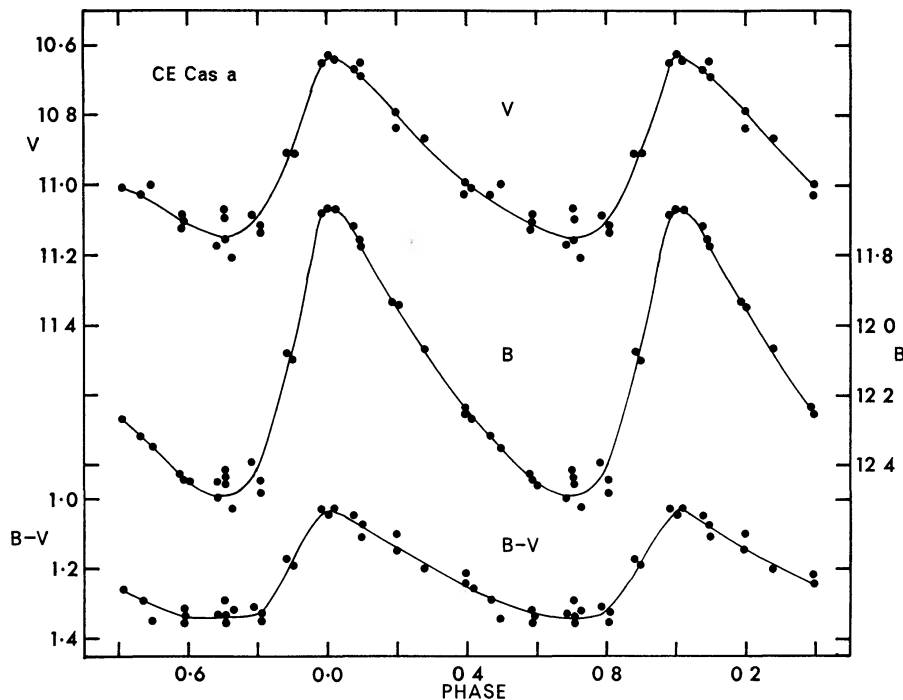


FIG. 1.—Light and color curves for CE Cas a from data in the second half of Table 1

plotted. The photographic values, corrected in zero point from their provisional values, are listed in Tables 2 and 3, but are not plotted. The mean difference between the systems is zero, but the scatter is naturally somewhat greater for the photographic data.

The deviations of the photoelectric data about the mean curves of Figures 1 and 2 average less than ± 0.02 mag. We are convinced that this is due mainly to random errors in the initial photoelectric photometry of the combined light and not to our separation procedure, because the deviations of each component in B and V are tightly correlated at a given epoch.

The photometric parameters derived from Figures 1 and 2 are listed in Table 4. The mean magnitudes $\langle B \rangle$ and $\langle V \rangle$ and the mean color $\langle B - V \rangle$ were determined by averaging over the relevant intensity curves. Not tabulated, but recoverable from the data in Table 4, are the $\langle B \rangle - \langle V \rangle$ colors. These differ only slightly from $\langle B - V \rangle$ but have been used in the discussion of the P - L - C relation in § V.

The reddening and the resulting absorption values are those determined by Kraft (1961*b*) for CF Cas. The stars CE and CF Cas are in the same general region of the

TABLE 3
 PHOTOGRAPHICALLY DETERMINED B MAGNITUDES ON THE ADOPTED
 PHOTOELECTRIC SYSTEM

Plate	H.J.D. 2 430 000+	Quality	CE Cas <u>a</u> ¹⁾		CE Cas <u>b</u> ²⁾	
			Phase	V	Phase	V
PH-1234-S	5 695.788	FP	0.311	12.02	0.045	11.60
1247-S	695.997	G	0.352	12.07	0.092	11.65
1256-S	696.804	P	0.509	12.31	0.272	11.96
1266-S	696.987	G	0.544	12.32	0.313	12.12
1290-S	698.744	FG	0.886	12.10	0.705	12.53
1301-S	698.998	FG	0.936	11.84	0.762	12.45:
1303-S	699.802	FG	1.092	11.74	0.942	11.79
1310-S	699.993	G	1.129	11.75	0.984	11.61
1319-S	700.957	G	1.317	12.08	1.199	11.87
12-A	6 218.612	P	102.007	11.60:	116.766	12.34:
3030-S	426.845	G	142.511	12.31	163.253	11.97
3037-S	429.985	P	143.122	11.70:	163.954	11.64:
3038-S	429.987	FG	143.122	11.83	163.955	11.83
3047-S	436.762	F	144.440	12.39	165.467	12.44
3067-S	455.791	F	148.141	11.88	169.715	12.58
3072-S	456.011	G	148.184	11.90	169.765	12.50
3078-S	456.745	F	148.327	12.14	169.929	11.91
3091-S	457.019	F	148.380	12.17	169.990	11.57
3334-A	758.957	F	207.111	11.89	237.397	12.34
3349-A	783.975	FP	211.977	11.64	242.982	11.63
3365-S	815.781	F	218.164	11.79	250.083	11.55
3411-S	820.781	G	219.136	11.73*	251.199	11.88*
3422-S	847.715	FP	224.375	12.22*	257.212	11.97*
3693-S	7 204.718	G	293.817	12.40	336.913	12.02
4032-S	969.790	FP	442.633	12.49	507.714	12.56
4048-S	973.637	FP	443.381	12.38	508.573	12.49
4055-S	974.631	FP	443.571	12.56	508.795	12.59

* Mean of three exposures on one plate

1) Phase of V(max) computed from epoch $J.D._{\odot} = 2\ 435\ 694.189 + 5.1410583n$

2) Phase of V(max) computed from epoch $J.D._{\odot} = 2\ 435\ 695.586 + 4.4793014n$

cluster (cf. Sandage 1958*b*, Fig. 1), and the assumption of equal reddening must be nearly correct. But to obtain reddenings accurate to 0.01 mag requires new photometry.

The distance modulus of NGC 7790 is uncertain at this time by perhaps ± 0.3 mag. In Table 4 we have adopted $(m - M)_0 = 12.53$, which is the weighted mean of the original value of 12.80 (Sandage 1958*b*) and Becker's (1963) value of 14.10 for the apparent modulus based on his method A, where a photometric fit is made of both the

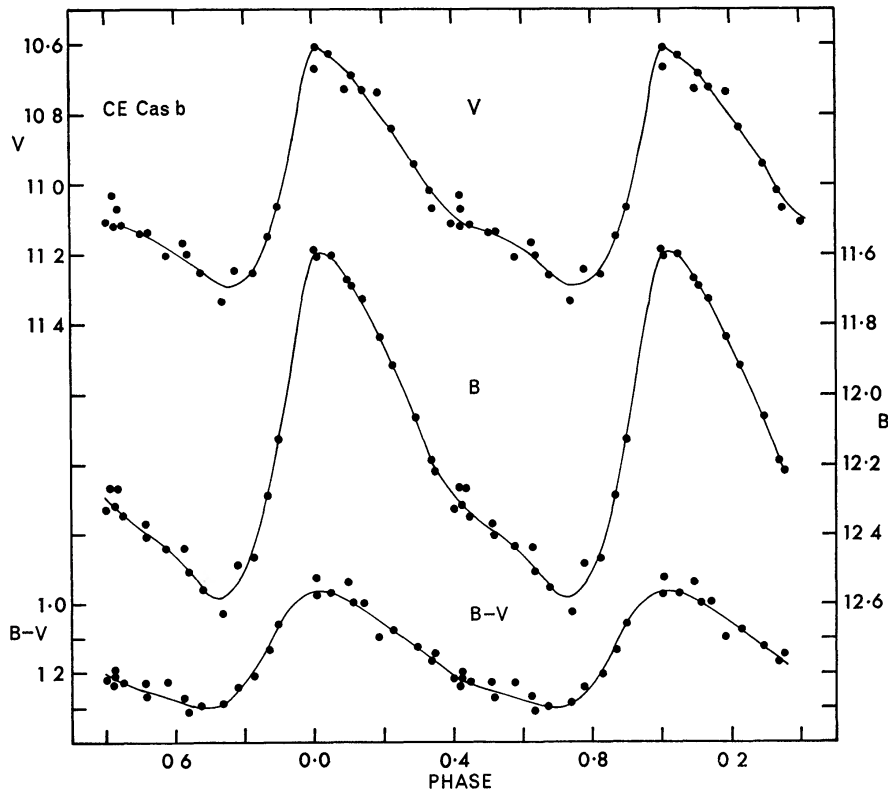


FIG. 2.—Same as Fig. 1 for CE Cas *b*

TABLE 4

PHOTOMETRIC PARAMETERS FOR CE CAS *a* AND CE CAS *b*

PARAMETER	CE CAS <i>a</i> *				CE CAS <i>b</i> †			
	Max	Min	Mean	Amp	Max	Min	Mean	Amp
<i>V</i>	10 63	11 15	10 92	0 52	10 61	11 29	10 99	0 68
<i>B</i>	11 67	12 49	12 12	0 82	11 585	12 59	12 11	1 005
<i>B - V</i>	1 03	1 345	1 21	0 315	0 96	1 30	1 14	0 34
V_0 ‡	8 965	9 485	9 255		8 945	9 625	9 325	
B_0 ‡	9 45	10 27	9 90		9 365	10 37	9 89	
$(B - V)_0$ ‡	0 475	0 79	0 655		0 405	0 745	0 585	
M_{V_0} §	- 3 565	- 3 045	- 3 275		- 3 585	- 2 905	- 3 205	
M_{B_0}	- 3 08	- 2 26	- 2 63		- 3 165	- 2 16	- 2 64	

* Epoch $V(\max) = 2435694.189 + 5.1410583n$

† Epoch $V(\max) = 2435695.586 + 4.4793014n$

‡ $E(B - V) = 0.555$ mag, $A_V = 1.665$ mag, $A_B = 2.22$ mag assumed.

§ $(m - M)_0 = 12.53$ assumed.

$(M_V, B - V)$ - and $(M_V, U - B)$ -diagrams, corrected to $(m - M)_0 = 12.44$ by Kraft's (1961*b*) color excess of $E(B - V) = 0.555$. Fitting the $U - B$ data has the advantage that the main-sequence slope is less steep than in $B - V$. Therefore, Becker's value has been given higher weight.

We regard our adopted modulus as the least satisfactory feature of the present work, primarily because the original photometry (Sandage 1958*b*) was done with the Mount Wilson 60-inch reflector with a less sensitive photometer than is now available. In addition, not enough of the faint main sequence was obtained for a first-class modulus determination. Because of the importance of CE and CF Cas we plan to remeasure the faint main sequence of NGC 7790 next season, at which time the $E(B - V)$ values can be strengthened.

Aside from the question of the absolute luminosities and unreddened colors, the errors of all other data in Table 4 are estimated to be near ± 0.02 mag. The random errors are considerably smaller because many individual points contribute to the light curves, but systematic errors are likely to be more important.

Our final values may be compared with those of Efremov and Kholopov (1965), who made a similar study using plates taken with the 28-inch reflector of the Sternberg Astronomical Institute. In both B and V , Efremov and Kholopov's magnitudes are brighter than ours by about 0.13 mag near maximum light. The $\langle B \rangle$ magnitudes agree with ours to within 0.01 mag, but their $\langle V \rangle$ values are brighter by 0.10 mag, a fact which shows that we both had similar difficulties for the yellow photographic plates.

Note added in proof, June 1, 1969.—After this paper was submitted, we became aware of a similar study by Smak (*Astr. Acta*, 16, 11, 1966), who obtained separate light curves in B and V for CE Cas a and b by photoelectric scanning with the 24-inch reflector at the Lick Observatory. Comparison of Smak's results (listed in his Table 4) with our Table 4 above, after adjustment to an adopted modulus of $(m - M)_0 = 12.53$, gives $\langle \Delta M_V(S - ST) \rangle = +0.045$ mag and $\langle \Delta M_B(S - ST) \rangle = +0.030$ mag for CE Cas a , and $\langle \Delta M_V(S - ST) \rangle = +0.025$ mag and $\langle \Delta M_B(S - ST) \rangle = 0.04$ mag for CE Cas b . The colors also show very good agreement. Smak obtains $\langle (B - V) \rangle_0$ of 0.63 and 0.58, while we find 0.655 and 0.585 for cases a and b , respectively.

III. PREDICTED AND OBSERVED PERIOD RATIOS FOR CE CAS a, b

The data in Table 4 show that the two components occupy different regions of the H-R diagram. Star a is brighter by 0.07 mag in V and redder by 0.07 mag in $B - V$. These differences are considerably larger than the errors and appear to be real. The data imply that the mean radius of a is larger than b , as required if $P \propto \rho^{-1/2}$ and $P_a > P_b$.

A quantitative check is possible if we know the slope of the relations $B - V = f(\log T_e)$ and $\Delta M_{bol} = g(B - V)$, the zero point not being required. For the most precise comparison we must also take into account the variation of Q across the instability strip. If a and b have the same mass, then

$$\frac{P_a}{P_b} = \left(\frac{R_a}{R_b} \right)^{1.5} \frac{Q_a}{Q_b}. \quad (1)$$

The ratio of the radii follow from the observed color and luminosity differences by adopting

$$\log T_e = \text{const.} - 0.175(B - V) \quad (2)$$

and

$$\Delta M_{bol} = \text{const.} - 0.322(B - V), \quad (3)$$

versions of which have been used by many authors following Oke's (1961) analysis of δ Cephei. A quite similar slope for the $(T_e, B - V)$ -relation has been obtained by Rodgers and Bell (1967, 1968*a, b*) from their studies of ι Car, S Mus, β Dor, and κ Pav.

Using equations (2) and (3) with $\Delta(B - V) = 0.07$ and $\Delta V = 0.07$, we obtain $\Delta M_{\text{bot}} = 0.092$ and

$$\frac{R_a}{R_b} = \left(\frac{L_a}{L_b}\right)^{1/2} \left(\frac{T_b}{T_a}\right)^2 = 1.102 ,$$

where L is the bolometric luminosity. Equation (1) then predicts

$$\frac{P_a}{P_b} = 1.156 \frac{Q_a}{Q_b} . \quad (4)$$

The quantity Q is expected to vary across the instability strip owing to the increasing importance of the transport of energy by convection as one proceeds toward lower temperatures across the H-R diagram. Increasing convection causes the effective polytropic index of the atmosphere to decrease from its radiative value toward its fully convective value of $n = 1.5$. Epstein (1950), summarizing the model calculations available in 1950, showed that Q increases with decreasing n . The result was confirmed and extended by Ledoux (1952) and Ledoux, Simon, and Bielaire (1955). Christy (1966) reaches the same conclusion by studying Q for each of his RR Lyrae models spread from the high-temperature to the low-temperature boundary of the strip. His results (equation on p. 134 of Christy 1966) show that Q varies slowly with T_e approximately as

$$\log Q \simeq \text{const.} - 0.2 \log T_e . \quad (5)$$

If the convective change across the strip is the same for Cepheids as for RR Lyrae stars, we can transform equation (5), using equation (2), into

$$\Delta \log Q \simeq 0.035 \Delta(B - V) , \quad (6)$$

which requires Q_a/Q_b to equal 1.006. Equation (4) then predicts that

$$\frac{P_a}{P_b} = 1.163 \pm 0.045 , \quad (7)$$

where the limits are calculated by assuming observational errors of ± 0.02 mag for the differences in V and $B - V$ between the components of CE Cas, each operating in the same direction to produce the extremes.

The observed period ratio is $P_a/P_b = 1.148$, which agrees with the prediction within the observational error. From this highly satisfactory agreement we conclude that the period difference between CE Cas a and b is fully explained by the different position of the stars within the strip. This result has no bearing on the reason why the components have different $(M_V, B - V)$ -values, but rather explains the period difference once the color and magnitude differences are given. The route by which the stars are mapped within the strip depends on the shape and time scale of the evolutionary track, as discussed in § VI.

A similar comparison of CF Cas and CE Cas can be made by using the data in Appendix A. The observations, together with equation (4), give $P_F/P_b = 1.047 \pm .040$, whereas the observed period ratio is $P_F/P_b = 1.088$. The result is shown in Figure 3, where lines of constant density are plotted in a highly enlarged portion of the instability strip. If the variation of Q is neglected, a procedure justified by the discussion in the next section, then these are lines of constant period.

The diagram not only serves as a confirmation that $P \propto \rho^{-1/2}$ across the strip in the neighborhood of $M_V \simeq -3$, but also serves as a test of the calibration of the P - L - C relation given in Paper I. The line placement was done by adopting the ridge-line P - L relation in Table A1 of the quoted reference, converting this to the H-R plane by the

ridge-line period-color relation given by

$$\langle B \rangle_0 - \langle V \rangle_0 = 0.264 \log P + 0.37, \quad (8)$$

and attaching the lines of constant period to the appropriate $M_{\langle B \rangle}$ and $M_{\langle V \rangle}$ values of Table A1. These lines were drawn with slopes of $\Delta M_B / \Delta(B - V) = 3.52$ and $\Delta M_V / \Delta(B - V) = 2.52$, which follow from the $P \propto \rho^{-1/2}$ assumption with constant Q by using the usual procedure (Sandage 1958*b*).

The absolute position of the stars in Figure 3 compared with the lines depends on the assumed modulus for NGC 7790. If we had adopted, not $(m - M)_0 = 12.53$, but rather, say 12.80, the stars would have moved 0.27 mag brighter. However, regardless of the absolute values, depending as they do on our previous calibration of the P - L - C relation, the *relative* positions of the stars and the lines are fixed by the color and magnitude observations. The agreement seems satisfactory. Figure 3 is a different representation of the test of the ratio of radii that was made in the first part of this section.

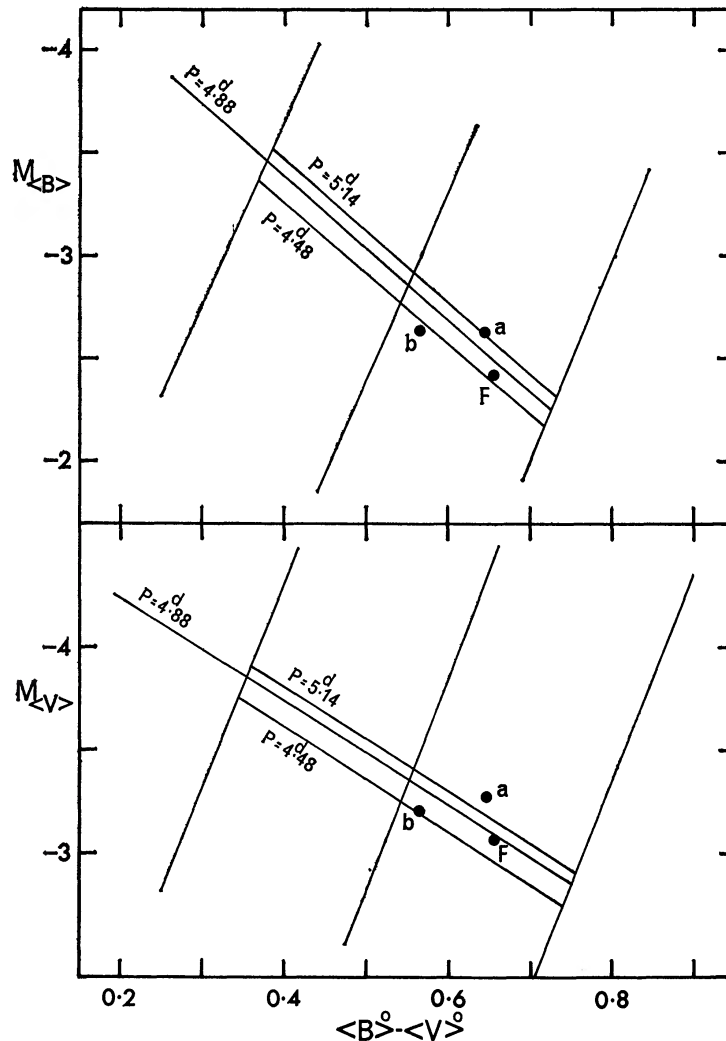


FIG. 3.—Section of the instability strip in the H-R diagram showing the lines of constant period according to the calibration of Paper I. CE Cas *a* and *b* and CF Cas are plotted from the data in Tables 4 and A2.

IV. EFFECT OF VARIABLE Q ON THE PERIOD-LUMINOSITY-COLOR RELATION

Our previous discussion (Sandage 1968*a*; Sandage and Tammann 1968) was based on $P\langle\rho\rangle^{1/2} = Q$. Because this relation has been challenged (Ferne 1967*c*), we wish to point out that the equation is quite general, applying to all types of mechanical systems in periodic motion under the control of gravity. It holds for large structures (e.g., bridges and telescopes) where the mean density is calculated from some appropriate characteristic length describing the system as a whole. It also holds for stellar configurations, such as binary stars and stars rotating near the point of instability, and even for the oscillation of the Universe itself, where

$$P\langle\rho\rangle^{1/2} = \left(\frac{3\pi}{G}\right)^{1/2} \left(\frac{q_0}{2q_0 - 1}\right)^{3/2} \text{ cgs units .}$$

However, the values of Q differs widely between these systems, although it generally shows a smaller variation among configurations of the same general type. The exact value must be calculated from the mass distribution of each.

For Cepheids, Q is expected to vary both across (i.e., as a function of $B - V$) and along (as a function of M_V or approximately P) the instability strip owing to nonhomologous changes of the atmospheres. A period dependence of Q in no way affects our previous analysis because such a variation only changes the *spacing* of the lines of constant period in the $(M_V, B - V)$ -plane and, therefore, the slope of the ridge-line P - L relation.¹ Because we adopted the slope from *observation* in Paper I, not from theory, our analysis is independent of any variation of Q with P . This is not, however, true of a variation of Q with $B - V$, as is now shown.

If Q varies across the strip, the slope of the constant-period lines will be affected, but the following argument shows the effect to be negligible. From $P\langle\rho\rangle^{1/2} = Q(P, B - V)$ it follows from equations (2), (3), and an adopted mass-luminosity relation that

$$M_V = -4.184(\log P - \log Q) + 2.52(\langle B \rangle - \langle V \rangle) + \text{const.} , \quad (9)$$

which is equation (1) of Paper I. If, in a first approximation, the variation of Q is expressed as

$$\log Q = h(B - V) + k \log P + m \quad (10)$$

equation (9) becomes

$$M_V = -4.18(1 - k) \log P + (2.52 + 4.18h)(\langle B \rangle - \langle V \rangle) + \text{const.} \quad (11)$$

The lines of constant period then have a slope

$$\frac{\Delta M_V}{\Delta(B - V)} = 2.52 + 4.18h . \quad (12)$$

If $h = 0.035$ by equation (6), the slope is 2.67, compared with 2.52 for constant Q . The corresponding slope in M_B is 3.67, compared with 3.52. The effect of these changes is below the limit of observational detection with the present data (cf. Figs. 2 and 3 of Paper I, or Fig. 6 given later in this paper).

The effect of $k \neq 0$ is seen by substitution of the ridge-line period-color relation of equation (8) in equation (11), giving the ridge-line P - L relation,

$$M_V = (-3.52 + 4.18k + 1.10h) \log P + \text{const.} \quad (13)$$

The term in k dominates the variable part of the coefficient of $\log P$, because that in h is negligible in the first approximation if h has a value close to that of equation (6). The

¹ The proof is given later in this section.

slope of the P - L relation then depends upon k as previously stated (see also Kraft 1961*b*). But, contrary to Fernie's (1967*c*) assertion that "to adopt the $P\rho^{1/2}$ relation as the fundamental basis of the method is unsatisfactory," the effect of $k \neq 0$ does not invalidate the method of Paper I. This is because, as previously stated, we established the slope of the ridge-line P - L relation from the *observations* of Cepheids in M31, the LMC, the SMC, and NGC 6822, and not from some form of equation (13). The $P\rho^{1/2}$ relation was used only to establish the slopes of the lines of constant period which, as we have just shown, are practically independent of any realistic variation of Q with $B - V$.

V. THE OBSERVED PERIOD-LUMINOSITY-COLOR RELATION

a) The Data

The adopted magnitudes and colors for the calibrating Cepheids in clusters and associations are listed in Tables 5 and 6 at mean and maximum light, respectively. Column (7) of Table 5 lists $\langle B \rangle_0 - \langle V \rangle_0$ at mean intensity, using the data in the Tonantzintla Catalogue (Mitchell *et al.* 1964) corrected by $E(B - V)$ in column (6) as derived in Paper I. Column (8) is calculated from the ridge-line ($P, B - V$)-relation of equation (8). Column (9) is the color residual, positive if the observed $\langle B \rangle_0 - \langle V \rangle_0$ is redder than the ridge-line relation. Columns (10) and (13) are the reddening-free absolute magnitudes obtained by using $A_V = 3E(B - V)$ and $A_B = 4E(B - V)$ and the adopted moduli of column (5) as in Paper I. It should be emphasized that the resulting M_V and M_B values are independent of the assumed absorption-to-reddening values as long as the same values were used to correct the *apparent* moduli to $(m - M)_0$ values. Columns (11) and (14) give the ridge-line luminosities read graphically from our previous calibration (Paper I, Table 1A). Columns (12) and (15) give the magnitude residuals, R_i , positive if the star is observed to be fainter than the ridge-line value. Similar data are given in Table 6 for maximum light, where the ridge-line relations are taken from Paper I.

We have adopted $(m - M)_0 = 11.30$ for RS Pup in the Pup III association, obtained by combining Westerlund's (1963) modulus of $(m - M)_0 = 11.20$ (weight 1) with a new determination of $(m - M)_0 = 11.35$ (weight 2) from the $(M_V, U - B)$ -diagram. The value of $E(B - V) = 0.55$ is the mean of the two members of Pup III closest to RS Pup. This differs from Westerlund's value of $E(B - V) = 0.62$ which he obtained from Kraft's (1961*b*) mean period-color relation. But this method anticipates that the Cepheid lies on the ridge-line ($P, B - V$)-relation and therefore also on the ridge-line P - L relation. The star can then no longer be used to calibrate the $[R_i, \delta(B - V)]$ -relation in the full analysis of the P - L - C relation. New photometric parameters for RS Pup itself have been derived by using all available photoelectric observations listed in the Tonantzintla Catalogue. The relevant ones are listed in Tables 5 and 6.

For SU Cas we have adopted the modulus given by Racine (1968) and the reddening listed in Table A2 of Paper I.

Not listed in Tables 5 and 6 are l Car and α UMi, which Fernie (1967*a, b*) discusses as members of wide pairs. He derives absolute magnitudes from photometric parallaxes of the secondary components. His values are $M^0_{\langle V \rangle} = -5.9 \pm 0.3$, $M^0_{\langle B \rangle} = -4.8 \pm 0.3$ for l Car ($\log P = 1.552$), and $M^0_{\langle V \rangle} = -3.2 \pm 0.3$, $M^0_{\langle B \rangle} = -2.7 \pm 0.3$ for α UMi ($\log P = 0.600$), which agree very well with the previous P - L relation. However, the uncertainty of membership for l Car is so great that one accepts or rejects membership on the basis of the agreement. The star α UMi is unique owing to its abnormally small amplitude despite its place near the ridge line of the P - L relation. If it is unique in this property, it may be unique in others, and we chose not to use the star as a calibrator.

Figures 4 and 5 show the P - L data in $M^0_{\langle B \rangle}$ and $M^0_{\langle V \rangle}$ at mean and maximum light for the thirteen listed Cepheids. The ridge lines and boundaries are taken from Table A1 of Paper I, and CF Cas and CE Cas a, b are shown as open circles, RS Pup as a triangle, SU as an X , and l Car and α UMi as vertical crosses.

CE Cas	b	7790	4.48	0.651	12.53	0.555	0.565	0.54	+0.02	-3.205	-3.25	+0.045	-2.64	-2.77	+0.13
CF Cas	"	"	4.87	0.687	12.53	0.555	0.655	0.55	+0.10	-3.075	-3.345	+0.27	-2.42	-2.86	+0.44
CE Cas	a	"	5.14	0.711	12.53	0.555	0.645	0.56	+0.09	-3.275	-3.41	+0.135	-2.63	-2.92	+0.29
UY Per	h + x	"	5.36	0.730	11.90	0.98	0.58	0.56	+0.02	-3.54	-3.46	-0.08	-2.96	-2.96	0.00
VY Per	"	"	5.53	0.743	11.90	1.06	0.55	0.57	-0.02	-3.91	-3.50	-0.41	-3.36	-2.99	-0.37
U Sgr	M25	"	6.74	0.828	8.98	0.55	0.55	0.59	-0.04	-3.93	-3.72	-0.21	-3.37	-3.20	-0.17
DL Cas	129	"	8.00	0.903	11.28	0.50	0.70	0.61	+0.09	-3.84	-3.95	+0.11	-3.14	-3.40	+0.26
S Nor	6087	"	9.75	0.989	9.76	0.23	0.73	0.63	+0.10	-4.03	-4.16	+0.13	-3.30	-3.61	+0.32
VX Per	h + x	"	10.89	1.037	11.90	0.58	0.64	0.64	0.00	-4.34	-4.31	-0.03	-3.70	-3.76	+0.06
SZ Cas	"	"	13.62	1.134	11.90	0.88	0.61	0.67	-0.06	-4.71	-4.59	-0.12	-4.10	-4.02	-0.08
RS Pup	P III	"	41.38	1.617	11.30	0.55:	0.89:	0.80	+0.09	-5.95	-5.97	+0.02	-5.06	-5.20	+0.14

TABLE 5
PARAMETERS FOR 13 CALIBRATING CEPHEIDS AT MEAN LIGHT

1	2	3	4	5	6	7	8	9	10	11	12	13	14	15
Star	Cluster	P	log P	(m-M) ^o	E(B-V)	$\langle B \rangle_o - \langle V \rangle_o$	$\delta(B-V)$	$\delta(B-V)$	M(V) ^o	M(V) ^o	R _V	M(B) ^o	M(B) ^o	R _B
						Obs	Cal		Obs	Cal		Obs	Cal	
SU Cas	-	1.95	0.290	7.5	0.33	0.38	0.45	-0.07	-2.54	-2.30	-0.24	-2.16	-1.94	-0.22
EV Sct	6664	3.09	0.490	11.03	0.58	0.57	0.50	+0.07	-2.62	-2.83	+0.21	-2.05	-2.38	+0.33

TABLE 6
PARAMETERS FOR 13 CALIBRATING CEPHEIDS AT MAXIMUM LIGHT

Star	$B_{\max}^{\circ} - V_{\max}^{\circ}$		$\delta(B-V)$	$M_V^{\circ}(\max)$		R_V	$M_B^{\circ}(\max)$		R_B
	Obs	Cal		Obs	Cal		Obs	Cal	
SU Cas	-	-	-	-2.75	-	-	-2.34	-	-
EV Sct	0.48	0.32	+0.16	-2.87	-3.21	+0.34	-2.39	-2.88	+0.49
CE Cas <u>b</u>	0.42	0.39	+0.03	-3.585	-3.56	-0.02	-3.165	-3.18	+0.01
CF Cas	0.49	0.40	+0.09	-3.375	-3.65	+0.27	-2.885	-3.25	+0.36
CE Cas <u>a</u>	0.48	0.40	+0.08	-3.565	-3.73	+0.16	-3.08	-3.31	+0.23
UY Per	0.38	0.41	-0.03	-4.00	-3.77	-0.23	-3.62	-3.36	-0.26
VY Per	0.39	0.42	-0.03	-4.30	-3.81	-0.49	-3.91	-3.40	-0.51
U Sgr	0.36	0.43	-0.07	-4.27	-4.08	-0.19	-3.91	-3.65	-0.26
DL Cas	0.55	0.44	+0.11	-4.09	-4.33	+0.24	-3.54	-3.89	+0.35
S Nor	0.60	0.44	+0.16	-4.34	-4.59	+0.25	-3.74	-4.15	+0.41
VX Per	0.47	0.43	+0.04	-4.68	-4.73	+0.05	-4.21	-4.31	+0.10
SZ Cas	0.49	0.41	+0.08	-4.93	-5.03	+0.10	-4.44	-4.61	+0.17
RS Pup	0.62	0.45	+0.17	-6.41	-6.45	+0.04	-5.79	-6.00	+0.21

b) *The Lines of Constant Period*

Figure 6 shows that the magnitude residuals R_i read at constant period correlate with the color residuals in the expected sense. As in Paper I (Fig. 2), the slopes of the lines are given their theoretical values of 2.52 and 3.52. As was mentioned in § IV, lines with slopes of 2.67 and 3.67 for variable Q are nearly the same as those drawn in Figure 6, differing by only several widths of the drawn lines at $\delta(B - V) = \pm 0.1$ mag.

Stars in Figure 6 cover the period range from $1^{\text{d}}95$ (SU Cas) to $41^{\text{d}}38$ (RS Pup). Although there is no evidence that the slope of lines of constant P is a function of P , the observations may not eliminate the possibility that some slight dependence may exist. But it is certainly apparent that the *sign* of the slope of the lines is the same for long- and short-period Cepheids; that is, at a given period, fainter Cepheids are redder for all periods in the observed range $2^{\text{d}} \leq P \leq 125^{\text{d}}$. This is shown in the present sample over a smaller range of periods, but it is particularly evident from the many stars over the entire period range shown in Figure 2 of Paper I. The point is important because Fernie (1967c) predicts a sign change of the slope in his P - L relation. The observations disagree

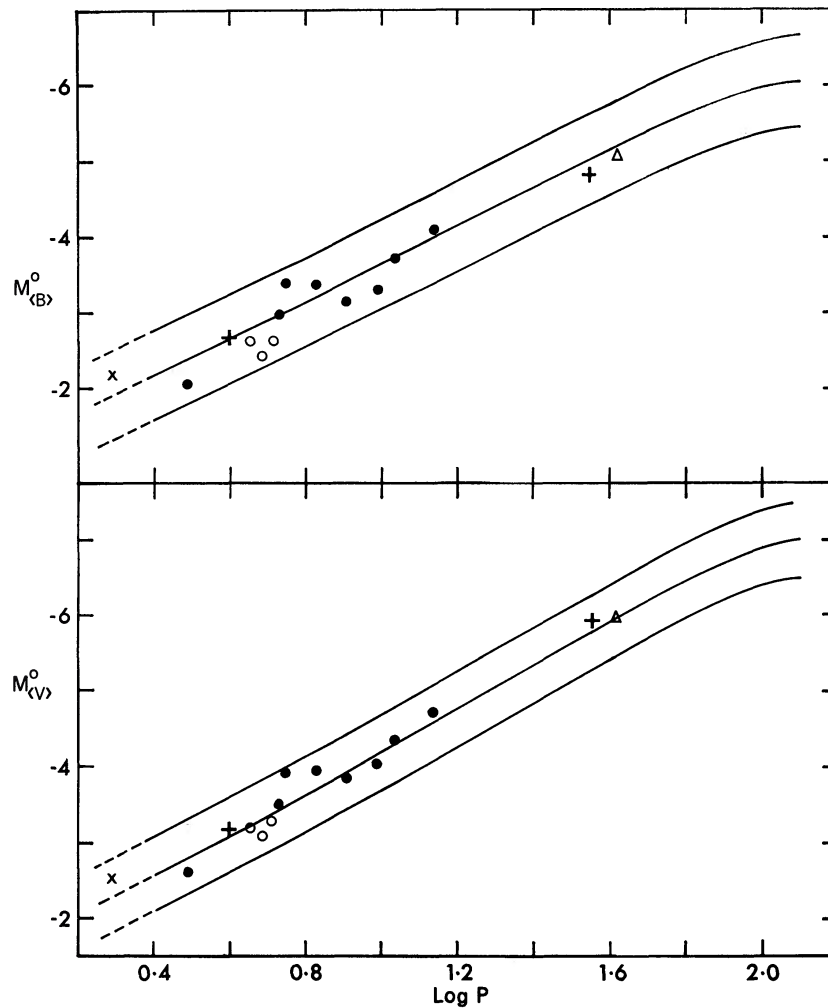


FIG. 4.—The P - L relation at mean light taken from Table A1 of Paper I. Data for the thirteen calibrating Cepheids are from Table 5. *Open circles*, CF Cas and CE Cas *a*, *b*; *triangle*, RS Pup, SU Cas and X; *vertical crosses*, 1 Car and α UMi. The remaining stars are shown as closed circles.

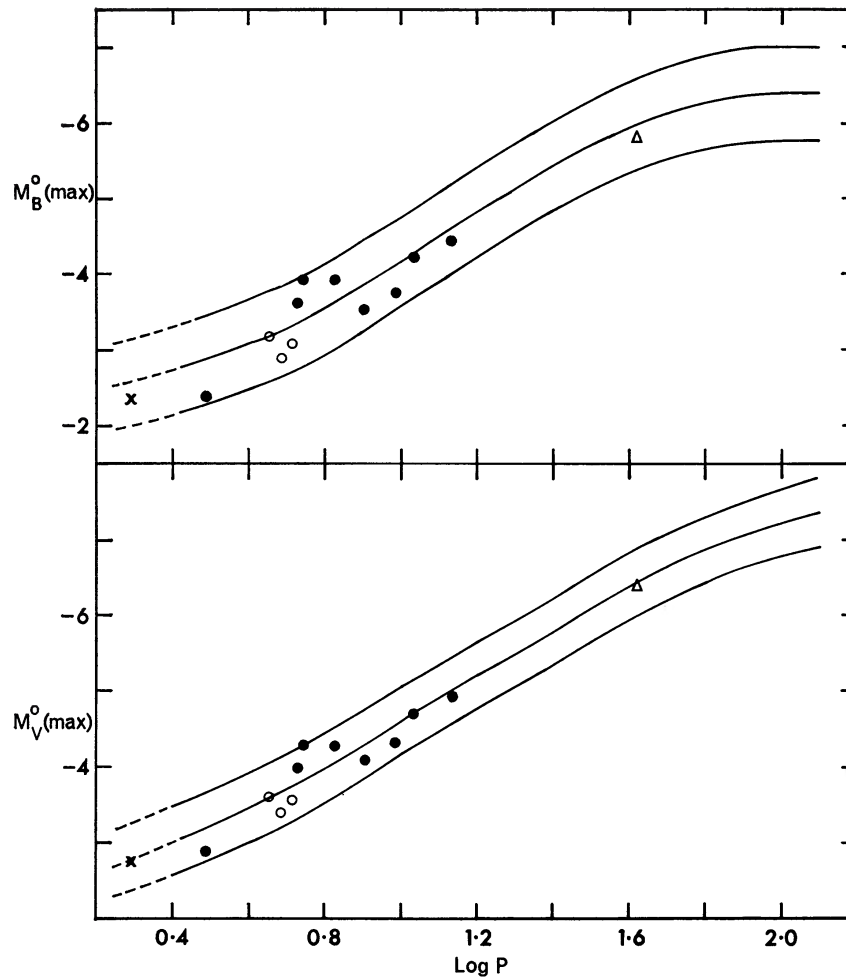


FIG. 5.—Same as Fig. 4 at maximum light

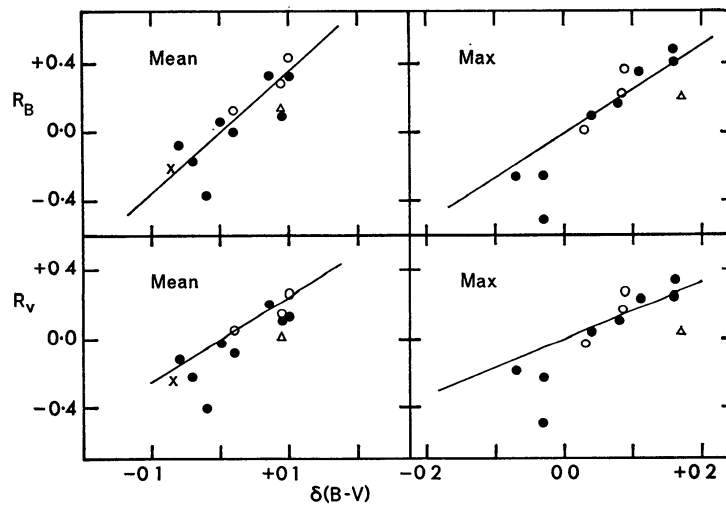


FIG. 6.—Correlation of magnitude residuals R_i from the ridge lines of Figs. 4 and 5 and the color residuals $\delta(B - V)$ relative to equation (8) for mean light and from the period-color relation in Paper I, for maximum light. Theoretical slope values of 3.52 and 2.52 have been assumed. The lines are placed through $R_i = 0$, $\delta(B - V) = 0$ to test the calibration in Paper I.

with Fernie's prediction. In addition, Fernie's very shallow period lines in the $(M_V, B - V)$ -plane (his Fig. 5) lead to a nearly dispersionless P - L diagram, again in disagreement with the observations (Fig. 1 of Paper I and Figs. 4 and 6 here).

In view of these discrepancies, we believe (1) that Fernie's equation (22), which predicts the unverified slope change, does not represent the available data; (2) that his lines of constant period are too shallow and that therefore the lack of scatter in his calculated P - L relation (his Fig. 4) is illusory; and (3) that the basis of his method of obtaining the color term (his eq. [20]) is unjustified.

c) The Calibration

The lines in Figure 6 have been drawn through $R_i = 0$, $\delta(B - V) = 0$. If the thirteen stars in Tables 5 and 6 were to define a calibration which differs from that listed in Table A1 of Paper I, there would be a systematic shift of the stars and the lines in Figure 6. Except for VY Per, which shows wide scatter on all four plots of this diagram and may not be at the adopted mean modulus of h and ψ Per (Schild 1967), Figure 6 suggests that our previous calibration is correct to at least ± 0.10 mag, barring systematic errors in the data of Tables 5 and 6.

Systematic errors rest, among other things, with the distance of the Hyades. The discussion on this point is the same as in Paper I. We can only state again that (1) Eggen's (1968) data on $(M_V, R - I)$ for nearby red dwarfs with $\pi > 0''.125$ compared with ten members of the Hyades show that Wayman, Symms, and Blackwell's (1965) modulus needs no change, the formal difference being 0.03 ± 0.14 (A.D.) mag; and (2) the supposed better agreement of $\pi(\text{trig.})$ for Hyades members with the change advocated by Hodge and Wallerstein (1966) is an illusion arising from a misunderstanding of relative and absolute parallaxes by these authors (Eggen 1967). We only mention the trigonometric-parallax argument here because so much emphasis has been placed on this aspect by other workers (Hodge and Wallerstein 1966; Wallerstein 1967; van Altena 1969). The differences under discussion are only $\Delta\pi \simeq 0''.005$. At this level, no argument via $\pi(\text{trig.})$ is secure because the absolute reference frame is itself uncertain by about this amount.

Although we believe that the systematic error arising from the Hyades question is negligibly small, it must be realized that the $(m - M)_0$ values for the relevant clusters and associations are not definitive for other reasons. New observations of the faint main sequence for each aggregate should be made to strengthen the present values.

An analytical test of the present calibration is possible by using the best-fitting linear equations describing the P - L - C relation. Figure 3, extended over the relevant range of the $(M_V, B - V)$ -plane by Table A1 of Paper I, results in Figure 7. Luminosities anywhere in this diagram are represented within a few hundredths of magnitude by

$$M_{(V)} = -3.425 \log P + 2.52(\langle B \rangle^\circ - \langle V \rangle^\circ) - 2.412 \quad (14)$$

in the range of $0.4 < \log P < 1.9$ and

$$M_{(B)} = -3.425 \log P + 3.52(\langle B \rangle^\circ - \langle V \rangle^\circ) - 2.412 \quad (15)$$

over the same period range, where the equations of the red and blue boundaries of the strip are

$$M_V = -10.9(\langle B \rangle^\circ - \langle V \rangle^\circ) + 5.36 \quad (16)$$

and

$$M_V = -10.9(\langle B \rangle^\circ - \langle V \rangle^\circ) + 0.02, \quad (17)$$

respectively. The ridge line is represented by

$$M_V = -10.9(\langle B \rangle^\circ - \langle V \rangle^\circ) + 2.67. \quad (18)$$

Other features of Figure 7 are discussed in § VI.

Equations (14) and (15) were used with the color data in column (7) of Table 5 to compute values of $M^0_{\langle V \rangle}$ and $M^0_{\langle B \rangle}$. Comparison with the observed values in columns (10) and (13) shows that $\langle \Delta M_V \rangle$ (Cal. - Obs.) = +0.07 mag if VY Per is included, and +0.05 mag if the star is ignored. We conclude that the calibration in Paper I, which was determined by graphical means, should be changed by ~ 0.05 mag toward brighter values on the basis of the present data using the analytical fit. This difference is not significant in view of the uncertainties in the cluster moduli involved. However, for completeness, the correction has been incorporated into the following equations, which represent our best approximation to the P - L - C relation for galactic Cepheids:

$$M_{\langle V \rangle} = -3.425 \log P + 2.52(\langle B \rangle^\circ - \langle V \rangle^\circ) - 2.459, \quad (19)$$

$$M_{\langle B \rangle} = -3.425 \log P + 3.52(\langle B \rangle^\circ - \langle V \rangle^\circ) - 2.459. \quad (20)$$

Table 7 shows the comparison of M_V (observed) and M_V (calculated from eq. [19]). If VY Per is excluded, the comparison gives

$$\langle \Delta M_V \rangle (\text{Cal.} - \text{Obs.}) = 0.00 \pm 0.064 \text{ (A.D.)}.$$

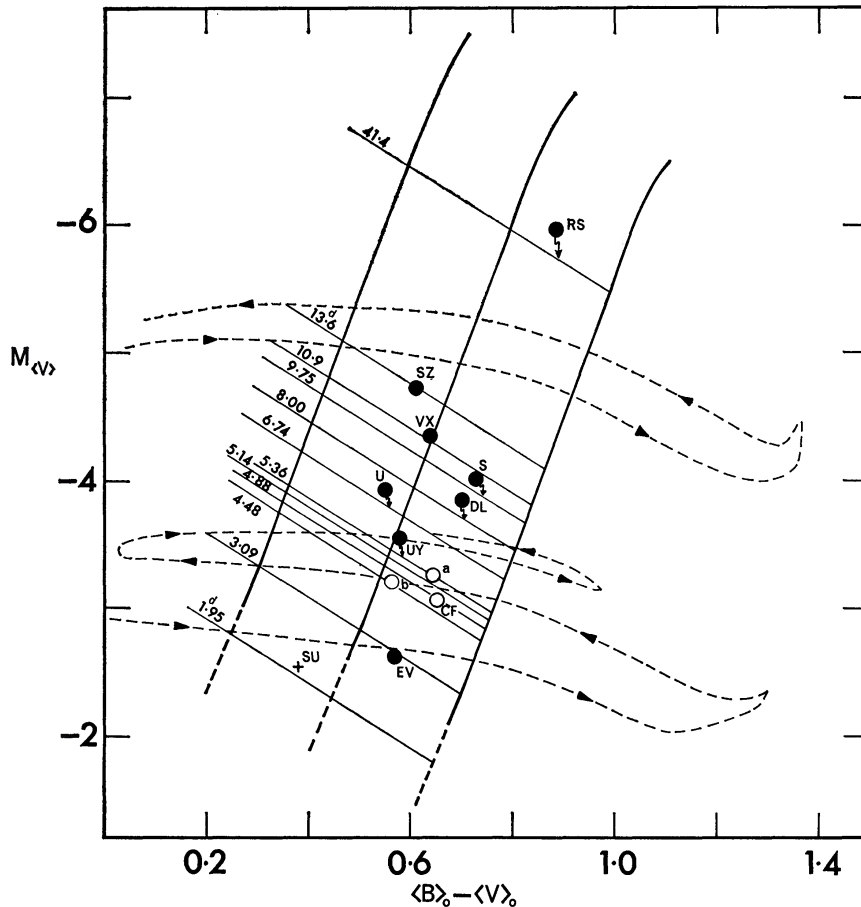


FIG. 7.—The instability strip defined in Paper I with lines of constant period for the observed stars. Data for the Cepheids are from Table 5. Iben's evolutionary tracks for stars of $5 M_{\odot}$ and $9 M_{\odot}$ computed with no mass loss are shown, but with the $5 M_{\odot}$ track shifted 0.2 mag brighter to pass through CE Cas *b* on the second crossing. The present calibration suggests that the lines of constant period should be placed 0.05 mag brighter than shown.

The average deviation is fortuitously small in view of uncertainties in the cluster distances upon which the M_V values of the calibrating stars are based.

The question of how universal equations (19) and (20) may be from galaxy to galaxy or in different parts of the same galaxy remains as a problem for future investigation. If the mean period-color distributions for Cepheids in the Magellanic Clouds actually differs from that in the Galaxy (Gascoigne and Kron 1965), one must expect a different $P-L-C$ relation. This need not imply a different position for the instability strip in the $(L_{bol}, \log T_e)$ -plane but could arise from (1) a different $(\log T_e, B - V)$ -relation, caused, for example, by temperature-independent color changes due to differences in blanketing, microturbulence, and electron pressure (e.g., Bell and Rodgers 1969), or (2) a biased distribution of Cepheids in the instability strip due, for example, to noncomplete and variable penetration of evolutionary tracks into the strip as a function of metal abundance. Such an effect is predicted by Hofmeister from her calculations (1967) of track position as a function of Z . In this latter case one would expect a difference in the slope

TABLE 7
COMPARISON OF M_V OBSERVED AND CALCULATED
FROM EQUATION (19)

Star	Cal M_V	Obs. M_V	Cal. - Obs.	Star	Cal. M_V	Obs. M_V	Cal. - Obs.
SU Cas . . .	-2 494	-2 54	+0 046	U Sgr	-3 909	-3 93	+0 021
EV Sct	-2.701	-2 62	-0 081	DL Cas . .	-3 788	-3 84	+0 052
CE Cas <i>b</i> . .	-3 265	-3 205	-0 060	S Nor	-4 006	-4 03	+0 024
CF Cas	-3 161	-3 075	-0 086	VX Per .	-4 398	-4 34	-0 058
CE Cas <i>a</i>	-3 269	-3 275	+0 006	SZ Cas	-4 806	-4 71	-0 096
UY Per	-3 497	-3 54	+0 043	RS Pup	-5 754	-5 95	+0 196
VY Per .	-3 618	-3 91	+0 292				

of the ridge-line $P-L$ relation coupled with a change in the ridge-line period-color relation such as recently observed by Gascoigne (1968) in the Magellanic Clouds. It is important that these effects be more completely understood if Cepheids are to be used as reliable distance indicators.

VI. THE EVOLUTION OF CF CAS AND CE CAS *a, b*

To first order, the results so far have not depended on the slopes of evolutionary tracks which feed the instability strip. The effect of nonhorizontal evolutionary tracks on $P(M_V, B = V, Q)$ is quite small (Kraft 1961*a*) considering the range of the computed slopes for all models now available. This follows because (1) an important parameter in the slope of the lines of constant period is the mass and (2) even those models which give large differences in luminosity at the blue and red boundaries of the instability strip require only slight differences in mass at a given M_V on the strip boundaries due to the steep mass-luminosity relation. The placing of the lines of constant density in Figure 7 is, therefore, nearly independent of the track slopes encountered in nature.

The same is not true, however, of the placing of the stars in Figures 3 and 7 which is determined directly by the *shape* of the evolutionary track. The star CE Cas *a* is brighter and redder than CE Cas *b*. One must know the direction of travel along the track to decide if component *a* and *b* is in the more advanced evolutionary state. Calculations by Hofmeister *et al.* (1964), Kippenhahn *et al.* (1965), Iben (1966*a, b*), and Forbes (1968) have shown that multiple crossings of the instability strip occur, and that the second crossing takes by far the longest time (Iben 1966*a*, Table 4). For a star of $5 M_{\odot}$,

Iben (1966*a*) shows that the ratio of times within a part of the instability strip of width $\Delta \log T_e = 0.02$ are $t_2/t_1 = 51.4$, $t_2/t_3 = 9.6$, and $t_2/t_4 = 32.4$ for the various crossings. Most Cepheids will, therefore, be observed on their second crossing, a result confirmed observationally by Kraft (1966).

There is, of course, the possibility that components a and b are on different crossings, but a calculation from the time ratios, with the condition that both stars are simultaneously within the strip, shows that the probability is small. A further check is afforded by comparing the observed luminosity difference with calculated differences for the various crossings. Figure 7 shows Iben's (1966*a*) track for a $5 M_\odot$ and a $9 M_\odot$ star, with the $5 M_\odot$ star moved upward by 0.2 mag to pass through CE Cas b on the second crossing, and shifted by $\Delta(B = V) = 0.05$, a shift corresponding to the main-sequence slope of $\Delta M_V / \Delta(B - V) = 4$ (the exact value is of no consequence in the present context). The track in $(M_{\text{bol}}, \log T_e)$ was transformed into $(M_V, B - V)$ by compromise temperature and ΔN_{bol} scales adopted from Popper (1959), Oke (1961), Harris (1963), and Johnson (1964). Some features of Figure 7 are similar to a diagram published by Kraft (1966, Fig. 1).

The differences in V -magnitude between the various crossings are $\Delta M_{1,2} = 0.53$ mag, $\Delta M_{2,3} = 0.35$ mag, and $\Delta M_{3,4} = 0.09$ mag. The observed difference between a and b is 0.07 mag. This leaves only the possibilities that a and b are on the same crossing (with then a slight discrepancy between Iben's prediction and the observations, as described below) or that a is on the fourth crossing and b on the third. The latter is highly improbable (1) on the basis of the time scales and (2) because the existence of the fourth crossing is somewhat hypothetical, depending on an uncertain cross-section of the $^{12}\text{C}(\alpha, p)^{16}\text{O}$ reaction.

Although the ΔM values from the models do, therefore, suggest that a and b are on the second crossing, we consider that the more certain of the arguments is given by the ratio of the crossing times. The values of ΔM between the various crossings depend on relatively subtle details of the model, and may therefore be somewhat less certain. From the available data we consider it likely, but not conclusively proved, that a and b are both on the second crossing, and that b is in a slightly more advanced evolutionary stage.

The remarkable fact is, *not* that a and b are in slightly *different* parts of the instability strip, but rather that they are *both* within the strip at all at the same time. The ratio of the time to cross the strip to the age of the cluster is small ($\Delta T/T \simeq 0.02$). Stars a and b must have followed nearly identical evolutionary tracks from the main sequence to reach the present condition of the pair. In the absence of other effects such as (1) rotation (Mark 1968), (2) mass loss (Forbes 1968), or (3) slightly different times of formation on the main sequence, the restriction on the initial main-sequence mass ratio is severe for both stars to be at nearly the same place in the H-R diagram in this phase of very rapid evolution.

If we exclude for the moment the perturbing effects just mentioned, we can estimate the initial mass ratio which is required for b to lead a if the simplest evolutionary history has been followed. On the assumption that both stars started their main-sequence life at the same time and are both now in the instability strip a time T later, component b reached the same evolution stage as a along a very slightly brighter track in time $T - \Delta t$, where Δt is the time to travel from this stage to its presently observed more advanced position. If a and b follow homologous tracks which are only minutely displaced in luminosity, then

$$\frac{T - \Delta t}{T} = \frac{\mathfrak{M}_b L_a}{\mathfrak{M}_a L_b}, \quad (21)$$

where the luminosity ratio refers to any given homologous evolutionary stage. In particular, this ratio applies also to the initial main sequence, where the mass-luminosity relation has the form $L \propto \mathfrak{M}^3$. Equation (21) then becomes

$$\frac{\mathcal{M}_b}{\mathcal{M}_a} = \left(\frac{T}{T - \Delta t} \right)^{0.43} \simeq \left(1 + \frac{\Delta t}{T} \right)^{0.43} \quad (22)$$

for $\Delta t/T \ll 1$.

To close approximation, Δt is the time for b to move by $\Delta(B - V) = 0.07$ mag across the strip. Iben's data give $\Delta t \simeq 2 \times 10^5$ years, which follows by dividing the time to cross $\Delta T_e = 0.02$ by 1.2 (to compensate for our vertical shift of 0.2 mag) and then dividing by the ratio of $\Delta \log T_e = 0.02$ to $\Delta \log T_e = 0.0123$, which corresponds to $\Delta(B - V) = 0.07$ by equation (2). The age of NGC 7790 is $T \simeq 7 \times 10^7$ years (Iben 1966, Table 1, model 17 corrected by $(\mathcal{M}/L)_{7790}/(\mathcal{M}/L)_{\text{Iben}} = 0.88$ for the shifted track in Fig. 7). This gives, by equation (22),

$$\frac{\mathcal{M}_b}{\mathcal{M}_a} = 1.0012$$

and

$$\left(\frac{L_b}{L_a} \right)_{\text{m.s.}} = 1.004$$

from the mass-luminosity relation.

On the assumption of unperturbed evolution of ideal, equal-age nonrotating stars, the *maximum* mass ratio which stars of this luminosity can have if they are to appear simultaneously anywhere within the strip on the same crossing can be calculated. The extreme case is when one star is on the blue boundary and the other on the red. From Figure 7, one obtains the width of the strip at constant M_V as $\Delta(B - V) \simeq 0.50$ mag, or $\Delta \log T_e = 0.088$ by equation (2). Iben's time scale, adjusted to this width and to the luminosity of CE Cas b , gives $\Delta t = 1.5 \times 10^6$ years, which, by equation (22) gives $\mathcal{M}_1/\mathcal{M}_2 = 1.007$ and $L_1/L_2 = 1.02$. Any greater mass ratio will cause one star to lead the other at a rate so much faster that both cannot be within the strip on the second crossing at the same time.

But these mass ratios may be unrealistic. At least two other possibilities exist for the early evolutionary history of each star. (a) If the analysis of Mark (1968) applies to stars of $\sim 5 \mathcal{M}_\odot$, then, even if a and b have identical masses and were deposited on the main sequence at the same time T , they would leave the main sequence at different times if their rotational velocities differ. Stars with high rotation stay on the main sequence for longer times than stars of the same mass with lower rotation. This would relax the stringent mass ratios calculated by equation (22). (b) Stars a and b might not have been deposited on the main sequence at the same time but might, because of differences in initial mass or some other parameter, have taken *slightly* different Hyashi times for initial contraction. If so, the calculation of mass ratios made above would no longer hold. (c) Mass loss may occur within the Cepheid instability strip itself, in which case the present position of components a and b would have a more complicated interpretation than we have given, and again the calculation of the initial $\mathcal{M}_a/\mathcal{M}_b$ would not apply.

That some complicating phenomenon has taken place is suggested by the slight disagreement of the observed luminosities of a and b compared with those predicted by Iben's track in Figure 7. This diagram shows Iben's track slopes toward *brighter* luminosities from right to left. The tracks without mass loss that were predicted by Hofmeister *et al.* (1964), Kippenhahn *et al.* (1965), and Henyey (quoted by Forbes 1968) all rise in the same sense by about 0.06 mag in the relevant color interval. However, the observations show a to be 0.07 mag brighter than b . The discrepancy of 0.13 mag is greater than our estimated observational errors of ± 0.02 mag and appears to be real.

Either our observations have larger systematic errors than we have estimated, or the tracks with no mass loss do not describe the situation of CE Cas a and b . It is interesting to note that Forbes (1968) shows that tracks with mass loss have a reversed slope on the second and third crossings which is of the right order to explain the observed data.

Until the complicating factors of rotation, age spread in reaching the initial main se-

quence, and mass loss are sorted out, one cannot explain with certainty the observed relative positions of CE Cas *a* or *b* or, indeed, CF Cas in Figure 7. But it remains a remarkable fact that *a* and *b* are in the same very narrow stage of evolution, no matter what the cause. That this is a rare phenomenon is evident from (1) the stringency of the theoretical requirements on the initial L_a/L_b and M_a/M_b put by the short time scale of the Cepheid phase, and (2) the observational fact that CE Cas is the only double Cepheid known.

It is a pleasure to thank O. J. Eggen for critically reading the manuscript. Discussions with A. W. Rodgers and S. C. B. Gascoigne are gratefully acknowledged. One of us (G. A. T.) is grateful to Dr. H. W. Babcock and the Staff Members of Mount Wilson and Palomar Observatories for their hospitality during his visits in Pasadena. He acknowledges that this work was supported in part by the Swiss Science Foundation.

APPENDIX A

NEW PHOTOMETRIC DATA FOR CF CASSIOPEIAE

Table A1 lists twenty new photoelectric *UBV* measurements of CF Cas obtained with the 60- and 200-inch reflectors. These data are plotted in Figure A1 as closed circles. The previously

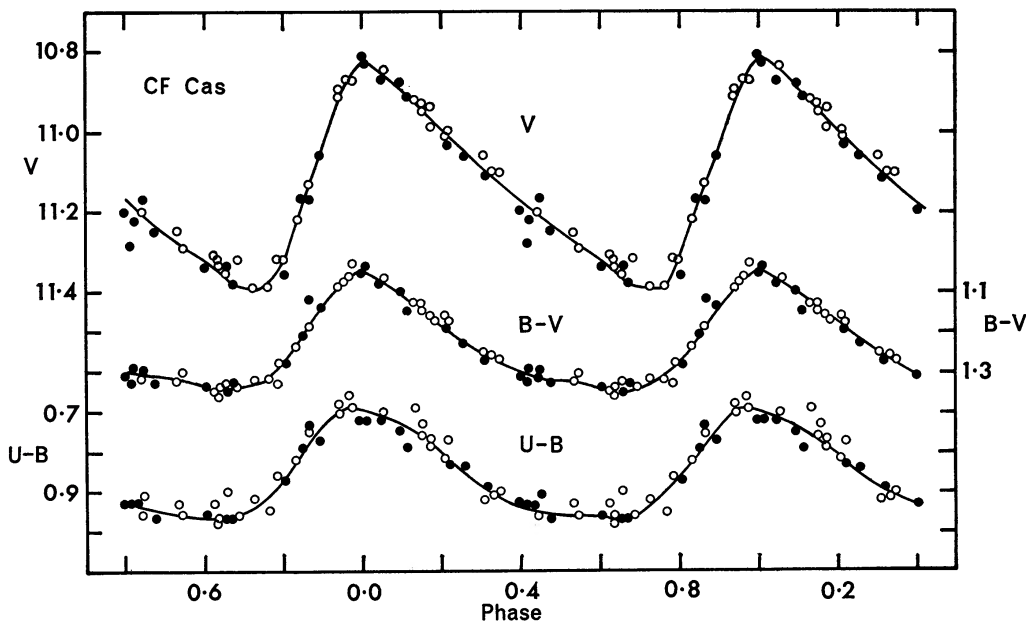


FIG. A1.—Light and color curve for CF Cas. *Open circles*, early data published previously

published values (Sandage 1958*b*) are shown as open circles. All data were phased by H.J.D. of $V(\max) = 2437104.954 + 4^d87522n$, where the period is the same as previously adopted. The fact that there is no systematic deviation of the closed circles from the open circles shows that the adopted period needs no correction.

We do not confirm the revision to the period suggested by Payne-Gaposchkin and Gaposchkin (1963). Adopting their period would cause a total phase difference of $\Delta\phi = 0.078$ from the phase calculated here over the interval of 2706^d.8 covered by the present and previous observations. Such a shift, which would be quite evident in Figure A1, does not occur.

New photometric parameters for CF Cas, derived from the combined data, are given in Table A2.

TABLE A1
NEW PHOTOMETRIC DATA FOR CF CAS

Date	J.D. _☉ 2 430 000 +	Phase*	V	B-V	U-B
1960 June 18/19	7 104.954	0.000	10.81	1.05	0.72
20/21	106.978	0.416	11.28:	1.33:	0.93:
Aug 16/17	164.010	12.114	10.91	1.15	0.79
17/18	165.003	12.318	11.11	1.27	0.89
Sept 23/24	201.939	19.894	11.06	1.14	0.77
24/25	202.918	20.095	10.88	1.10	0.75
27/28	205.743	20.674	11.38	1.33	0.97
28/29	206.677	20.866	11.17	1.12	0.74
1961 Jan 12/13	312.640	42.601	11.34	1.34	0.96
13/14	313.633	42.804	11.36	1.28	0.87
14/15	314.626	43.008	10.83	1.04	0.72
15/16	315.635	43.215	11.03	1.19	0.83
16/17	316.640	43.421	11.22	1.29	0.93
Oct 11/12	584.675	98.400	11.20	1.31	0.93
1962 Dec 26/27	8 025.636	188.850	11.17	1.21	0.79
27/28	026.607	189.049	10.87	1.08	0.72
28/29	027.629	189.258	11.06	1.23	0.84
29/30	028.704	189.479	11.25	1.33	0.97
1963 Dec 10/11	374.703	260.450	11.17	1.30	0.91
11/12	375.708	260.656	11.34	1.35	0.97

* Phase computed from epoch $V(\max) = 2\ 437\ 104.954 + 4.87522n$

TABLE A2
PHOTOMETRIC PARAMETERS FOR CF CAS*

Parameter	Max.	Min	Mean	Amplitude
V	10 82	11 39	11 12	0 57
B	11 865	12 715	12 33	0 85
$B - V$	1 035	1 34	1.23	0 305
V_0^\dagger	9 155	9 725	9 455	
B_0^\dagger	9 645	10 495	10 11	
$(B - V)_0^\dagger$	0 48	0 785	0 65	
$M_{V_0}^\ddagger$	- 3 375	- 2 805	- 3 075	
$M_{B_0}^\ddagger$	- 2 885	- 2 035	- 2 42	

* Epoch $V(\max) = 2437104.954 + 4.87522n$

† $E(B - V) = 0.555$, $A_V = 1.665$, $A_B = 2.22$ assumed

‡ $(M - M)_0 = 12.53$ assumed.

APPENDIX B

PHOTOMETRIC DATA FOR QX CASSIOPEIAE

Table B1 lists new photoelectric measurements made with the 60- and 200-inch telescopes. The last six entries are observations made by R. J. Dickens, which he has kindly permitted us to use. The new data (open circles), together with those previously reported (Sandage 1958*b*, closed circles), are plotted in Figure B1, phased according to H.J.D. of primary minimum = $2435682.938 + 6^d00471n$. The orbit has a moderate eccentricity, and the stars differ slightly in surface brightness.

The binary is likely to be a cluster member and may be important in strengthening the

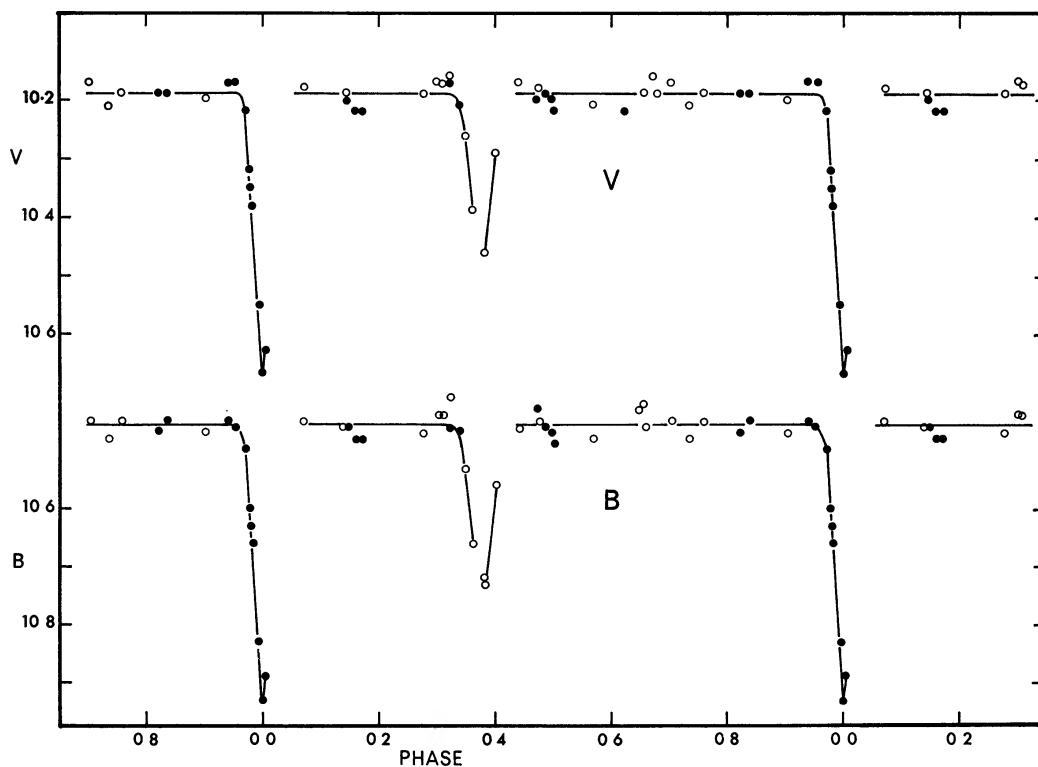


FIG. B1.—Light curves for QX Cas. *Closed circles*, data published previously

TABLE B1
NEW PHOTOMETRIC DATA FOR QX CAS

Date	H.J.D. 2 430 000 +	Phase*	V	B-V	U-B
1960 Sept 28/29	7 206.682	253.758	10.19	0.26	-0.59
1961 Jan 12/13	312.642	271.404	10.29	0.27	-0.64
13/14	313.635	.569	10.21	0.27	-0.64
14/15	314.626	.735	10.21	0.27	-0.64
15/16	315.637	.903	10.20	0.27	-0.63
16/17	316.644	272.071	10.18	0.27	-0.62
Oct 11/12	584.678	316.708	10.17	0.28	-0.62
1962 Dec 26/27	8 025.642	390.144	10.19	0.27	-0.60
27/28	026.603	.304	10.17	0.27	-0.60
27/28	026.625	.308	10.17	0.27	-0.62
27/28	026.713	.323	10.16	0.25	-0.62
28/29	027.633	.476	10.18	0.27	-0.60
29/30	028.719	.657	10.19	0.27	-0.59
1963 Dec 10/11	374.707	448.276	10.19	0.28	-0.62
11/12	375.712	.443	10.17	0.29	-0.59
1965 Oct31/Nov 1	9 065.690	563.350	10.26	0.27	-0.63
	065.758	.361	10.39	0.27	-0.62
	065.886	.382	10.46	0.26	-0.62
	065.887	.382	10.47	0.27	-0.63
Nov 2/3	067.631	.673	10.16	0.27	-0.61
	067.677	.680	10.19:	0.23:	-0.61

* Phase computed from H.J.D. 2 435 682.938 + 6^d.00471n

calibrations of mass, radius, and temperature of luminous stars when good curves of light and velocity are available. Double lines have been observed on two spectrograms by D. S. Hall (1967). He comments on photographic data by Erleksova *et al.* (1960).

The star QX Cas has a close companion of separation $\sim 3''$. The light of the companion was included in the diaphragm used for the photoelectric measurements, and the data in Table B1 refer to the combined light. We estimate the magnitude of the companion to be $B \simeq 14.5$, $V \simeq 13.1$. Corrections to the data of Table B1 to obtain QX alone are therefore $\sim +0.02$ mag at maximum, $+0.03$ at primary eclipse, and $+0.03$ at secondary eclipse in B , and $+0.10$, 0.16 , and 0.13 mag, respectively, for the same phases in V .

REFERENCES

- Becker, W. 1963, *Zs. f. Ap.*, **57**, 117.
 Bell, R. A., and Rodgers, A. W. 1969, *M.N.R.A.S.*, **142**, 161.
 Christy, R. F. 1966, *Ap. J.*, **144**, 134.
 Efremov, Y. N., and Kholopov, P. N. 1965, *Astr. Circ.*, U.S.S.R., No. 326.
 Eggen, O. J. 1967, *Ann. Rev. Astr. and Ap.*, **5**, 105.
 ———. 1968, *Ap. J. Suppl.*, **16**, 49.
 Epstein, I. 1950, *Ap. J.*, **112**, 6.
 Erleksova, G. E., Lange, G. A., Perova, N. B., Satanova, E. A., Kholopov, P. N., and Tsarevsky, G. S. 1960, *Variable Stars*, **13**, 41.
 Fernie, J. D. 1967a, *A. J.*, **71**, 732.
 ———. 1967b, *ibid.*, **72**, 708.
 ———. 1967c, *ibid.*, 1327.
 Forbes, J. E. 1968, *Ap. J.*, **153**, 495.
 Gascoigne, S. C. B. 1968, *Proc. Astr. Soc. Australia*, **1**, 96.
 Gascoigne, S. C. B., and Kron, G. E. 1965, *M.N.R.A.S.*, **130**, 333.
 Hall, D. S. 1967, *Pub. A.S.P.*, **79**, 630.
 Harris, D. L. 1963, in *Stars and Stellar Systems*, Vol. 3, ed. K. Aa. Strand (Chicago: University of Chicago Press), p. 263.
 Hodge, P. W., and Wallerstein, G. 1966, *Pub. A.S.P.*, **78**, 411.
 Hofmeister, E. 1967, *Zs. f. Ap.*, **65**, 164.
 Hofmeister, E., Kippenhahn, R., and Weigert, A. 1964, *Zs. f. Ap.*, **60**, 57.
 Iben, I. 1966a, *Ap. J.*, **143**, 483.
 ———. 1966b, *ibid.*, 505.
 Johnson, H. L. 1964, *Bol. Obs. Tonantzintla y Tacubaya*, **3**, 305.
 Kippenhahn, R., Thomas, H., and Weigert, A. 1965, *Zs. f. Ap.*, **61**, 241.
 Kraft, R. P. 1961a, *Ap. J.*, **133**, 39.
 ———. 1961b, *ibid.*, **134**, 616.
 ———. 1966, *ibid.*, **144**, 1008.
 Kuiper, G. P. 1935, *Pub. A.S.P.*, **47**, 121.
 ———. 1951, in *Astrophysics*, ed. J. A. Hynek (New York: McGraw-Hill Book Co.), chap. 8.
 Ledoux, P. 1952, *Bull. Soc. Roy. Sci. Liège*, **21**, 408.
 Ledoux, P., Simon, R., and Bielaire, J. 1955, *Ann. d'Ap.*, **18**, 65.
 Mark, J. W.-K. 1968, *Ap. J.*, **154**, 627.
 Mitchell, R. I., Iriarte, B., Steinmetz, D., and Johnson, H. L. 1964, *Bol. Obs. Tonantzintla y Tacubaya*, **3**, 153.
 Oke, J. B. 1961, *Ap. J.*, **134**, 214.
 Payne-Gaposchkin, C., and Gaposchkin, S. 1963a, *Pub. A.S.P.*, **75**, 171.
 ———. 1963b, *ibid.*, **75**, 193.
 Popper, D. M. 1959, *Ap. J.*, **129**, 647.
 Racine, R. 1968, *A. J.*, **73**, 588.
 Rodgers, A. W., and Bell, R. A. 1967, *M.N.R.A.S.*, **136**, 91.
 ———. 1968a, *ibid.*, **138**, 1.
 ———. 1968b, *ibid.*, **139**, 175.
 Sandage, A. 1958a, *Ap. J.*, **127**, 513.
 ———. 1958b, *ibid.*, **128**, 150.
 Sandage, A., and Gratton, L. 1963, *Star Evolution* (New York: Academic Press), p. 11.
 Sandage, A., and Tammann, G. A. 1968, *Ap. J.*, **151**, 531 (Paper I).
 Schild, R. 1967, *Ap. J.*, **148**, 449.
 van Altena, W. 1969, *Ap. J.* (in press).
 Wallerstein, G. 1967, *Pub. A.S.P.*, **79**, 317.
 Waymann, P. A., Symms, L. S. T., and Blackwell, K. C. 1965, *R.O.B.*, No. 98.
 Westerlund, B. E. 1963, *M.N.R.A.S.*, **127**, 71.